

Au–Tl Linear Chains as Lewis Acids toward $[\text{Au}(\text{C}_6\text{X}_5)_2]^-$ Metalloligands: The First Anionic Heteropolymetallic Chains

Eduardo J. Fernández,^{*,§} Antonio Laguna,^{*,‡} José M. López-de-Luzuriaga,[§] Manuel Montiel,[§] M. Elena Olmos,[§] and Javier Pérez[§]

Departamento de Química, Grupo de Síntesis Química de La Rioja, UA-CSIC, Complejo Científico Tecnológico, Universidad de la Rioja, 26006 Logroño, Spain, and Departamento de Química Inorgánica, Instituto de Ciencia de Materiales de Aragón, Universidad de Zaragoza-CSIC, 50009 Zaragoza, Spain

Received December 10, 2004

The heteropolynuclear complexes $[\text{AuTlR}_2]_n$ ($\text{R} = 3,5\text{-C}_6\text{Cl}_2\text{F}_3, \text{C}_6\text{Cl}_5$) can react with $[\text{AuR}_2]^-$ metalloligands leading to products of stoichiometry $\{\text{NBu}_4[\text{Tl}_2\{\text{Au}(\text{C}_6\text{Cl}_5)_2\}\{\mu\text{-Au}(\text{C}_6\text{Cl}_5)_2\}_2]\}_n$ (**2**), $\{\text{NBu}_4[\text{Tl}\{\text{Au}(3,5\text{-C}_6\text{Cl}_2\text{F}_3)_2\}_2]\}_n$ (**3**), or $\{\text{NBu}_4[\text{Tl}\{\text{Au}(\text{C}_6\text{Cl}_5)_2\}\{\text{Au}(3,5\text{-C}_6\text{Cl}_2\text{F}_3)_2\}]\}_n$ (**4**), which have incorporated a half (**2**) or one (**3**, **4**) additional gold center per thallium atom. These complexes are the first anionic heteropolymeric chains built via unsupported metal–metal interactions, which are considered to be responsible for the luminescent behavior. These compounds display a strong visible luminescence at room temperature and at 77 K in the solid state under UV excitation, which is sensitive to the structural arrangement of metals as well as to the perhalophenyl group bonded to gold(I). The crystal structures of three of these complexes have been determined by X-ray diffraction crystallography, showing bridging (**2**) or terminal (**3**, **4**) $[\text{AuR}_2]^-$ fragments bonded to the thallium centers of the principal Au/Tl chain and an almost planar environment for the thallium atoms.

Introduction

Among the methods that lead to the synthesis of supramolecular architectures one of the best known is the linkage of polyatomic anions with metal centers that act as Lewis acids, leading to products that display finite or polymeric structures.¹

In this context, in previous papers we have demonstrated the capability of $[\text{AuR}_2]^-$ ($\text{R} = \text{C}_6\text{F}_5, \text{C}_6\text{Cl}_5$) to form one-dimensional polymeric chains when treated with Tl^+ salts.² These are built by means of $\text{Au}\cdots\text{Tl}$ interactions, although long $\text{X}\cdots\text{Tl}$ ($\text{X} = \text{halogen}$) contacts seem also to contribute to the stability of those systems. A noticeable characteristic of these products is that the Tl^+ centers still keep their acid properties, despite still having a lone pair, and, thus, they further react with neutral O-, N-, or S-donor ligands such as OPPh_3 , tetrahydrofuran, acetylacetone, 1,10-phenantroline, 2,2'- and 4,4'-bipyridine, and tetrahydrothiophene,³ leading to polymeric structures in the solid state built also by means of short gold–thallium interactions, but showing also the presence of secondary interactions with the

halogen atoms of neighbor perhalophenyl groups. It is worth noting that the calculated strength of the Au–Tl interaction is about 276 kJ/mol, consisting of 20% van der Waals and 80% ionic interactions. From these observations it can be deduced that one electron-rich $[\text{AuR}_2]^-$ unit is not enough to neutralize the electrostatic charge of one Tl^+ center and the presence of additional electronic sources through covalent or van der Waals interactions (neutral ligands or halogens, respectively) is still needed.

In this regard, we wondered if the acid Tl^+ atoms present in these heteropolynuclear chains are able to incorporate a second basic $[\text{AuR}_2]^-$ anion, which implies its behavior as metalloligand and which would give rise to anionic heteronuclear infinite chains. Such a reaction would be favored by the presence of perhalophenyl groups capable of bridging two different metal centers through the formation of 3c-2e bonds or showing additional metal \cdots halogen interactions. Recently, we have shown the capability of 3,5- $\text{C}_6\text{Cl}_2\text{F}_3$ to act as bridging group in heterometallic Ag/Au systems,⁴ and it has also

* To whom correspondence should be addressed. E-mail: alaguna@posta.unizar.es; eduardo.fernandez@dq.unirioja.es.

§ Universidad de la Rioja.

‡ Universidad de Zaragoza-CSIC.

(1) (a) Hawthorne, M. F.; Zheng, Z. *Acc. Chem. Res.* **1997**, *30*, 267. (b) Hawthorne, M. F. *Pure Appl. Chem.* **1994**, *66*, 245. (c) Wuest, J. D. *Acc. Chem. Res.* **1999**, *32*, 81. (d) Vaugeois, J.; Simard, M.; Wuest, J. D. *Coord. Chem. Rev.* **1995**, *95*, 55.

(2) (a) Fernández, E. J.; Laguna, A.; López-de-Luzuriaga, J. M.; Monge, M.; Montiel, M.; Olmos, M. E.; Pérez, J. *Organometallics* **2004**, *23*, 774. (b) Fernández, E. J.; López-de-Luzuriaga, J. M.; Monge, M.; Olmos, M. E.; Pérez, J.; Laguna, A.; Mohamed, A. A.; Fackler, J. P., Jr. *J. Am. Chem. Soc.* **2003**, *125*, 2022.

(3) (a) Fernández, E. J.; Laguna, A.; López-de-Luzuriaga, J. M.; Mendizábal, F.; Monge, M.; Olmos, M. E.; Pérez, J. *Chem. Eur. J.* **2003**, *9*, 456. (b) Fernández, E. J.; López-de-Luzuriaga, J. M.; Monge, M.; Montiel, M.; Olmos, M. E.; Pérez, J.; Laguna, A.; Mendizábal, F.; Mohamed, A. A.; Fackler, J. P., Jr. *Inorg. Chem.* **2004**, *43*, 3573. (c) Fernández, E. J.; Jones, P. G.; Laguna, A.; López-de-Luzuriaga, J. M.; Monge, M.; Olmos, M. E.; Pérez, J. *Inorg. Chem.* **2002**, *41*, 1056. (d) Fernández, E. J.; Laguna, A.; López-de-Luzuriaga, J. M.; M. Olmos, E.; Pérez, J. *Dalton Trans.* **2004**, 1801. (e) Crespo, O.; Fernández, E. J.; Jones, P. G.; Laguna, A.; López-de-Luzuriaga, J. M.; Mendía, A.; Monge, M.; Olmos, E. *Chem. Commun.* **1998**, 2233. (f) Fernández, E. J.; Jones, P. G.; Laguna, A.; López-de-Luzuriaga, J. M.; Monge, M.; Montiel, M.; Olmos, M. E.; Pérez, J. *Z. Naturforsch. B* **2004**, in press.

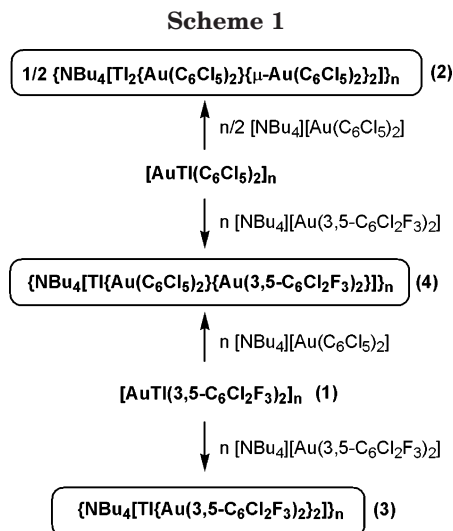
been shown that C_6Cl_5 usually shows $Tl\cdots Cl$ interactions in the polymeric Au/Tl systems mentioned above.^{2b,3a-d}

Taking all these considerations into account, we decided to treat the polymeric materials $[AuTl(C_6X_5)_2]_n$ with $Q[Au(C_6X_5)_2]$ ($C_6X_5 = C_6Cl_5, 3,5-C_6Cl_2F_3$) in different molar ratios and in a noncoordinating solvent, such as toluene, to avoid its possible coordination to the thallium(I) atoms. As we expected, the reaction occurs with the incorporation of one or half a bis(perhalophenyl)aurate(I) fragment to each Tl^+ center of the chain depending on the C_6X_5 group, resulting in the formation of anionic heteropolymetallic chains. It is worth noting that, although some anionic gold(I),⁵ silver(I),^{5a,b} or platinum(II)⁶ polymeric chains, as well as cationic gold(I)⁷ or platinum(II)⁸ one-dimensional polymers, have already been described, these are the first examples of anionic heteropolynuclear infinite chains reported to date.

Results and Discussion

Synthesis and Characterization. By reacting equimolecular amounts of $NBu_4[Au(C_6Cl_5)_2]$ and $TIPF_6$ in tetrahydrofuran, the precursor complex $[AuTl(C_6Cl_5)_2]_n$ is obtained according to the literature procedure.^{2b} Similarly, $[AuTl(3,5-C_6Cl_2F_3)_2]_n$ (**1**) is obtained as a white solid with analytical and spectroscopic data in agreement with the proposed stoichiometry (see Experimental Section).

To test the acid properties of the thallium centers of these complexes, in a first stage we treated complexes $[AuTlR_2]_n$ ($R = C_6Cl_5, 3,5-C_6Cl_2F_3$) with equimolecular amounts of the tetrabutylammonium bis(perhalophenyl)aurate containing the same aryl group as the neutral precursor. In both cases, the initial suspension of the polymeric materials in toluene slowly changes its appearance, and after 1 h of stirring, the addition of *n*-hexane led to complexes of different stoichiometry depending on the aryl group present in the product: $\{NBu_4[Tl_2\{Au(C_6Cl_5)_2\}\{\mu-Au(C_6Cl_5)_2\}_2]\}_n$ (**2**) or $\{NBu_4[Tl\{Au(3,5-C_6Cl_2F_3)_2\}_2]\}_n$ (**3**). In the case of complex **2**, both its analytical data and the presence of unreacted $NBu_4[Au(C_6Cl_5)_2]$ in the *n*-hexane solid residuals point out that the molar ratio of the starting materials should be 2:1. According to this, when the same reaction is carried out in a 2:1 molar ratio, complex **2** is obtained as the only product in a higher yield. By contrast, when the reaction involving $[AuTl(3,5-C_6Cl_2F_3)_2]_n$ and $NBu_4[Au(3,5-C_6Cl_2F_3)_2]$ is carried out



in this last molar ratio, complex **3** and unreacted **1** are isolated from the reaction medium (see Scheme 1). The analytical and spectroscopic data of both complexes agree with the proposed stoichiometries. The presence of NBu_4^+ was confirmed in their IR, 1H NMR, and mass (ES+) spectra, in which the parent peak appears at $m/z = 242$. Their IR spectra in Nujol mulls show, among others, absorptions arising from the C_6Cl_5 ⁹ and 3,5- $C_6Cl_2F_3$ ⁴ groups bonded to gold(I) at 836 and 614 for **2** and at 1587, 1561, 1047, and 775 cm^{-1} for **3**, respectively. The ^{19}F NMR of complex **3** displays two resonances due to the two types of fluorine atoms of the perhalophenyl groups, which appear at the same chemical shift as in the starting material.

A second stage in this synthesis was centered on the study of the influence of the perhalophenyl groups in the starting materials in order to test the possibility of exchange of aryl groups between the molecules. Thus, we carried out the reaction of each heteroatomic neutral complex with the $NBu_4[AuR_2]$ compound containing the other aryl group. Surprisingly, both reactions lead to the same product, $\{NBu_4[Tl\{Au(C_6Cl_5)_2\}\{Au(3,5-C_6Cl_2F_3)_2\}_2]\}_n$ (**4**), even when the molar ratio changes from 1:1 (as in complex **3**) to 2:1 (as in complex **2**) (see Scheme 1).

In this case, its analytical and spectroscopic data are also in accordance with the proposed stoichiometry. Its IR, 1H NMR, and mass (ES+) spectra confirm again the presence of the cation in the complex. In addition, its IR spectrum in Nujol mulls shows the above absorptions arising from the C_6Cl_5 ⁹ and 3,5- $C_6Cl_2F_3$ ⁴ groups bonded to gold(I) at 837 and 612 (C_6Cl_5) and at 1587, 1560, 1047, and 776 cm^{-1} (3,5- $C_6Cl_2F_3$). The ^{19}F NMR of complex **4** is similar to that registered for **3**.

Crystal Structures. The crystal structures of complexes **2–4** (see Figures 1–3 and Tables 1–4) have been determined from crystals obtained by slow diffusion of hexane in a saturated solution of the complex in toluene. They can be described as infinite chains formed via unsupported $Au\cdots Tl$ interactions in the range 3.0559–(4)–3.1678(4) (**2**), 3.0329(5)–3.1196(5) (**3**), and 3.0108–(3)–3.0914(2) Å (**4**) (similar to those observed in most of the polymeric species with unsupported $Au\cdots Tl$

(4) Fernández, E. J.; Laguna, A.; López-de-Luzuriaga, J. M.; Monge, M.; Montiel, M.; Olmos, M. E.; Pérez, J.; Puelles, R. C.; Sáenz, J. C. Manuscript submitted for publication.

(5) (a) Rawashded-Omary, M. A.; Omary, M. A.; Patterson, H. H. *J. Am. Chem. Soc.* **2000**, *122*, 10371. (b) Rawashded-Omary, M. A.; Omary, M. A.; Patterson, H. H.; Fackler, J. P., Jr. *J. Am. Chem. Soc.* **2001**, *123*, 11237. (c) Cramer, R. E.; Smith, D. W.; VanDoorne, W. *Inorg. Chem.* **1998**, *37*, 5895. (d) Leznoff, D. B.; Xue, B.-Y.; Batchelor, R. J.; Einstein, F. W. B.; Patrick, B. O. *Inorg. Chem.* **2001**, *40*, 6026. (e) Stender, M.; Olmstead, M. M.; Balch, A. L.; Rios, D.; Attar, S. J. *J. Chem. Soc., Dalton Trans.* **2003**, 4282.

(6) Williams, J. M.; Schultz, A. J.; Underhill, A. E.; Carneiro, K. In *Extended Linear Chain Compounds*; Miller, J. S., Ed.; Plenum Press: New York, 1982; Vol. 1, p 73.

(7) (a) White-Morris, R. L.; Olmstead, M. M.; Jiang, F.; Balch, A. L. *Inorg. Chem.* **2002**, *41*, 2313. (b) Lee, Y.; Eisenberg, R. *J. Am. Chem. Soc.* **2003**, *125*, 15059.

(8) Stork, J. R.; Olmstead, M. M.; Balch, A. L. *Inorg. Chem.* **2004**, *43*, 7508.

(9) Usón, R.; Laguna, A.; Laguna, M.; Manzano, B. R.; Tapia, A. *Inorg. Chim. Acta* **1985**, *101*, 151.

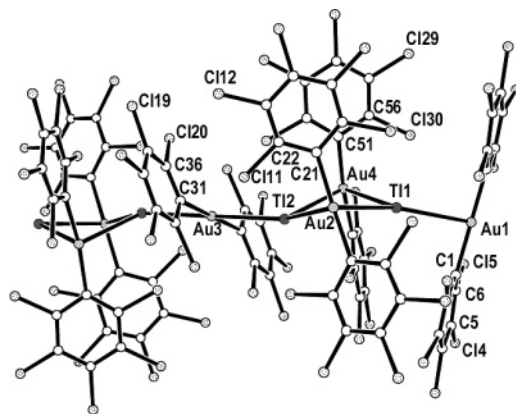


Figure 1. Structure of the anion of complex **2** with the labeling scheme of the atom positions. H atoms are omitted for clarity.

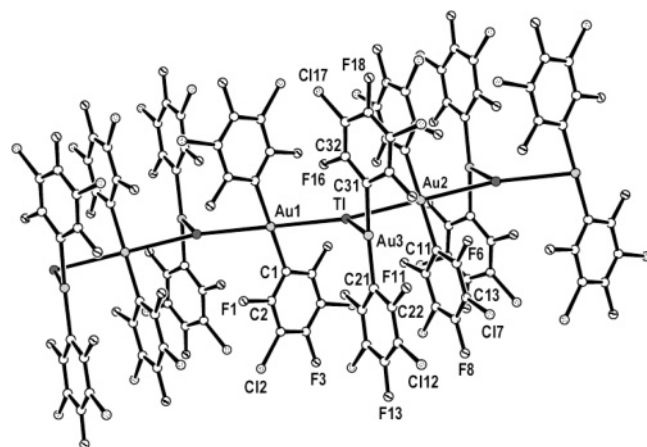


Figure 2. Structure of the anion of complex **3** with the labeling scheme of the atom positions. H atoms are omitted for clarity.

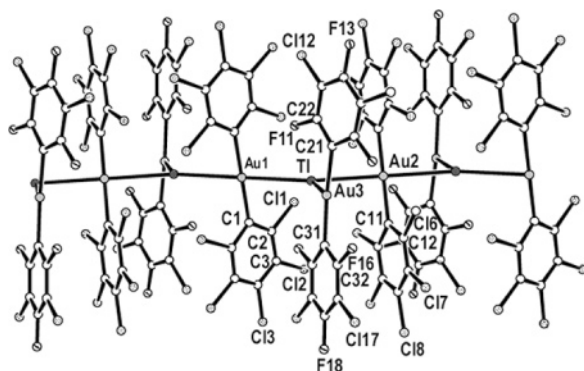


Figure 3. Structure of the anion of complex **4** with the labeling scheme of the atom positions. H atoms are omitted for clarity.

interactions^{2,3}), which have incorporated a half (**2**) or one (**3**, **4**) additional $[\text{AuR}_2]^-$ ($\text{R} = \text{C}_6\text{Cl}_5$, $3,5\text{-C}_6\text{Cl}_2\text{F}_3$) fragment per thallium to the chain also via new $\text{Au}\cdots\text{Tl}$ unsupported interactions of similar length, thus resulting in the formation of the first examples of heteropolymetallic anionic chains described to date. The presence of aurophilic interactions can be ruled out, since the shortest metal–metal distance between gold(I) centers $[\text{Au}(2)\text{–Au}(3) = 3.520 \text{ \AA} (\mathbf{3})]$ is longer than twice its van der Waals radius (3.32 \AA). The different number of bis(aryl)aurate(I) anions incorporated to the

chain, which influences their bonding mode as bridging (Figure 4) or terminal metalloligands (Figure 5), is the responsible for the differences found in their crystal structures. Thus, the anionic chain of complex **2** can also be seen as an association of loosely bound butterfly Au_2Tl_2 clusters that are joined together by an anionic $[\text{Au}(\text{C}_6\text{Cl}_5)_2]^-$ fragment. The bond lengths and angles within the tetranuclear core of the butterfly are similar to those found in the Au–Tl butterfly-type loosely bound clusters previously reported,¹⁰ although the gold(I) centers of the tetranuclear units display a more distorted linear environment (C–Au–C : $166.7(2)^\circ$ and $168.6(2)^\circ$ in **2**) than in the previous examples (C–Au–C angles between $173.7(2)^\circ$ and $178.0(2)^\circ$),¹⁰ while the $[\text{Au}(\text{C}_6\text{Cl}_5)_2]^-$ fragments that join two Au_2Tl_2 units contain perfectly linearly two-coordinate gold atoms (if the intermetallic interactions are not considered). The M–M'–M angles within the Au_2Tl_2 units are also slightly different than in the previous cases, showing wider Tl–Au–Tl ($82.658(10)^\circ$ and $84.881(11)^\circ$) and narrower Au–Tl–Au ($92.312(11)^\circ$ and $91.659(11)^\circ$) angles, avoiding the formation of $\text{Tl}\cdots\text{Tl}$ interactions (Tl–Tl : 4.14 \AA) that are present in the rest of loosely bound butterfly Au_2Tl_2 clusters (Tl–Tl : $3.6027(6)\text{–}3.7152(4) \text{ \AA}$).¹⁰ Finally, the coordination sphere of the Tl atoms in this complex is almost planar, with a sum of angles around the Tl(I) of 359.3° and 352.4° , although the Au–Tl–Au angles of the Au_2Tl_2 cores are always narrower than the others. This implies that, surprisingly, the stereoactivity of the inert pair, usually stereochemically active,¹¹ is not apparent in this case.

In the cases of complexes **3** and **4**, each thallium(I) center of the polymetallic Au/Tl chain binds a terminal $[\text{Au}(3,5\text{-C}_6\text{Cl}_2\text{F}_3)_2]^-$ fragment (see Figure 5), with the C_6Cl_5 groups in the case of complex **4** forming part of the chain, which runs parallel to the crystallographic x axis. As in the case of complex **2**, the Au(I) atoms of the main chain display a perfectly linear environment (if the intermetallic interactions are not considered), while those present in the terminal $[\text{Au}(3,5\text{-C}_6\text{Cl}_2\text{F}_3)_2]^-$ units show a distorted environment, with C–Au–C angles of $168.9(4)^\circ$ (**3**) and $170.1(2)^\circ$ (**4**). The coordination sphere of the Tl atoms in these two complexes is, as in complex **2**, almost planar (sum of Au–Tl–Au angles of Tl(I) of 358.5° (**3**) and 359.6° (**4**)) with a nearly T-shape environment for each thallium center (see Tables 3 and 4). As in **2**, the stereoactivity of the inert pair, usually stereochemically active,¹¹ is not apparent either in this case.

Finally, the presence of $\text{Tl}\cdots\text{Cl}$ ($3.180(2)\text{–}3.663(2) \text{ \AA}$), $\text{Au}\cdots\text{Cl}$ ($3.149(2)\text{–}3.385(2) \text{ \AA}$), $\text{Tl}\cdots\text{F}$ ($2.926(8)\text{–}3.352(1) \text{ \AA}$), and $\text{Au}\cdots\text{F}$ ($2.991(8)\text{–}3.106(4) \text{ \AA}$) interactions between halogen atoms of the same chain probably contributes to the stability of the system.

Optical Properties. On the other hand, and in addition to their interesting structures, all the complexes (**1–4**) are luminescent at room temperature and at 77 K in the solid state but not in solution. Their UV–vis spectra in deoxygenated tetrahydrofuran are similar

(10) (a) Fernández, E. J.; López-de-Luzuriaga, J. M.; Monge, M.; Olmos, M. E.; Pérez, J.; Laguna, A. *J. Am. Chem. Soc.* **2002**, *124*, 5942. (b) Fernández, E. J.; López-de-Luzuriaga, J. M.; Olmos, M. E.; Pérez, J.; Laguna, A.; Lagunas, M. C. Manuscript submitted for publication.

(11) Kristiansson, O. *Eur. J. Inorg. Chem.* **2002**, 2355–2361, and references therein.

Table 1. Details of Data Collection and Structure Refinement for Complexes 2, 3, and 4

	2	3	4
chemical formula	C ₅₂ H ₃₆ Au ₃ Cl ₃₀ N ₁₂ Tl ₂	C ₄₀ H ₃₆ Au ₂ Cl ₈ F ₁₂ N ₁₂ Tl	C ₄₀ H ₃₆ Au ₂ Cl ₁₄ F ₆ N ₁₂ Tl
cryst habit	yellow prism	green prism	yellow prism
cryst size/ mm	0.3 × 0.1 × 0.08	0.5 × 0.3 × 0.25	0.25 × 0.18 × 0.1
cryst syst	triclinic	monoclinic	monoclinic
space group	<i>P</i> $\bar{1}$	<i>P</i> 2 ₁ / <i>n</i>	<i>P</i> 2 ₁ / <i>n</i>
<i>a</i> /Å	15.0212(2)	12.2466(1)	12.0920(1)
<i>b</i> /Å	15.1626(2)	28.2173(4)	28.5736(3)
<i>c</i> /Å	17.7726(3)	15.1129(2)	15.4221(2)
α /deg	73.664(1)	90	90
β /deg	72.235(1)	108.925(1)	107.365(1)
γ /deg	79.629(1)	90	90
<i>V</i> /Å ³	3679.55(9)	4940.19(10)	5085.66(9)
<i>Z</i>	2	4	4
<i>D</i> /g cm ⁻³	2.471	2.206	2.272
<i>M</i>	2737.96	1640.60	1739.30
<i>F</i> (000)	2528	3064	3256
<i>T</i> /°C	-100	-100	-100
2 θ _{max} /deg	56	47	56
μ (Mo K α)/mm ⁻¹	11.451	9.687	9.706
no. reflns measd	53 187	39 819	42 397
no. unique reflns	17 410	7316	12 086
<i>R</i> _{int}	0.0572	0.0561	0.0532
<i>R</i> [<i>F</i> > 2 σ (<i>F</i>)] ^a	0.0422	0.0480	0.0400
<i>wR</i> [<i>F</i> ² , all reflns] ^b	0.0925	0.1757	0.0896
no. of reflns used	17410	7316	12086
no. of params	800	584	584
no. of restraints	226	170	166
<i>S</i> ^c	1.016	1.223	1.056
max. residual electron density/e Å ⁻³	1.984	1.327	1.604

^a $R(F) = \sum ||F_o| - |F_c|| / \sum |F_o|$. ^b $wR(F^2) = [\sum \{w(F_o^2 - F_c^2)^2\} / \sum \{w(F_o^2)^2\}]^{0.5}$; $w^{-1} = \sigma^2(F_o^2) + (aP)^2 + bP$, where $P = [F_o^2 + 2F_c^2]/3$, and *a* and *b* are constants adjusted by the program. ^c $S = [\sum \{w(F_o^2 - F_c^2)^2\} / (n - p)]^{0.5}$, where *n* is the number of data and *p* the number of parameters.

Table 2. Selected Bond Lengths [Å] and Angles [deg] for Complex 2^a

Au(1)–C(1)	2.064(8)	Au(1)–Tl(1)	3.1001(3)
Au(2)–C(11)	2.055(8)	Au(2)–Tl(1)	3.1062(4)
Au(2)–C(21)	2.051(8)	Au(2)–Tl(2)	3.1678(4)
Au(3)–C(31)	2.054(7)	Au(3)–Tl(2)	3.0940(3)
Au(4)–C(41)	2.062(7)	Au(4)–Tl(1)	3.0842(4)
Au(4)–C(51)	2.074(7)	Au(4)–Tl(2)	3.0559(4)
C(1)–Au(1)–Tl(1)	88.47(18)	C(21)–Au(2)–C(11)	166.7(2)
C(1)#1–Au(1)–Tl(1)	91.53(18)	C(31)#2–Au(3)–C(31)	180.0
C(11)–Au(2)–Tl(1)	87.14(18)	C(41)–Au(4)–C(51)	168.6(2)
C(11)–Au(2)–Tl(2)	105.77(18)	Tl(1)–Au(2)–Tl(2)	82.658(10)
C(21)–Au(2)–Tl(1)	100.84(17)	Tl(2)–Au(3)–Tl(2)#2	180.0
C(21)–Au(2)–Tl(2)	85.98(18)	Tl(2)–Au(4)–Tl(1)	84.881(11)
C(31)–Au(3)–Tl(2)	96.59(18)	Au(1)–Tl(1)–Au(2)	158.203(13)
C(31)–Au(3)–Tl(2)#2	83.41(18)	Au(4)–Tl(1)–Au(1)	108.827(10)
C(41)–Au(4)–Tl(1)	92.7(2)	Au(4)–Tl(1)–Au(2)	92.312(11)
C(51)–Au(4)–Tl(1)	92.19(18)	Au(3)–Tl(2)–Au(2)	148.614(12)
C(41)–Au(4)–Tl(2)	95.16(18)	Au(4)–Tl(2)–Au(2)	91.659(11)
C(51)–Au(4)–Tl(2)	95.56(17)	Au(4)–Tl(2)–Au(3)	112.141(11)

^a Symmetry transformations used to generate equivalent atoms: #1 $-x+2, -y, -z-1$, #2 $-x+1, -y, -z$.

Table 3. Selected Bond Lengths [Å] and Angles [deg] for Complex 3^a

Au(1)–C(1)	2.060(14)	Tl–Au(1)	3.1196(5)
Au(2)–C(11)	2.077(15)	Tl–Au(2)	3.0329(5)
Au(3)–C(21)	2.058(13)	Tl–Au(3)	2.9704(7)
Au(3)–C(31)	2.065(14)		
C(1)–Au(1)–Tl	83.9(3)	C(11)–Au(2)–C(11)#2	180.0
C(1)#1–Au(1)–Tl	96.1(3)	C(21)–Au(3)–C(31)	168.9(4)
C(11)–Au(2)–Tl	93.6(3)	Au(2)–Tl–Au(1)	168.83(2)
C(11)#2–Au(2)–Tl	86.4(3)	Au(3)–Tl–Au(1)	117.89(2)
C(21)–Au(3)–Tl	97.8(3)	Au(3)–Tl–Au(2)	71.783(15)
C(31)–Au(3)–Tl	93.3(3)	Tl–Au(1)–Tl#1	180.0
C(1)#1–Au(1)–C(1)	180.0	Tl#2–Au(2)–Tl	180.0

^a Symmetry transformations used to generate equivalent atoms: #1 $-x+1, -y, -z$, #2 $-x, -y, -z$.

Table 4. Selected Bond Lengths [Å] and Angles [deg] for Complex 4^a

Au(1)–C(1)	2.046(6)	Tl–Au(1)	3.0914(2)
Au(2)–C(11)	2.043(6)	Tl–Au(2)	3.0108(2)
Au(3)–C(21)	2.043(7)	Tl–Au(3)	3.0317(3)
Au(3)–C(31)	2.052(6)		
C(1)–Au(1)–Tl	85.04(15)	C(11)#2–Au(2)–C(11)	180.0
C(1)#1–Au(1)–Tl	94.96(15)	C(21)–Au(3)–C(31)	170.1(2)
C(11)–Au(2)–Tl	92.46(15)	Au(2)–Tl–Au(1)	164.436(9)
C(11)#2–Au(2)–Tl	87.54(15)	Au(3)–Tl–Au(1)	119.329(9)
C(21)–Au(3)–Tl	92.85(17)	Au(2)–Tl–Au(3)	75.869(7)
C(31)–Au(3)–Tl	96.89(16)	Tl–Au(1)–Tl#1	180.0
C(1)#1–Au(1)–C(1)	180.0	Tl#2–Au(2)–Tl	180.0

^a Symmetry transformations used to generate equivalent atoms: #1 $-x, -y, -z+1$, #2 $-x+1, -y, -z+1$.

and fairly featureless, displaying only the characteristic high-energy absorptions assigned to transitions involving the perhalophenyl groups at 246, 267, and 274 nm

when the aryl group is 3,5-C₆Cl₂F₃ and 246, 267, 274, and 301 nm when C₆Cl₅ is present in the complex.^{2a} This behavior in solution seems to be in accordance with the



Figure 4. Polymetallic chain of complex **2** with the $[\text{Au}(\text{C}_6\text{Cl}_5)_2]^-$ anions acting as bridging metalloligands.

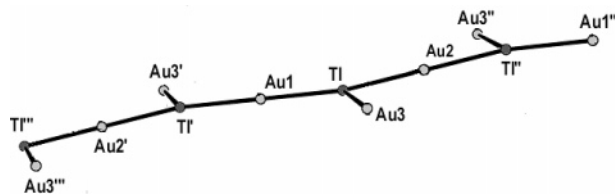


Figure 5. Polymetallic chain of complexes **3** and **4** with the $[\text{Au}(3,5\text{-C}_6\text{Cl}_2\text{F}_3)_2]^-$ anions acting as terminal metallo-ligands.

rupture of the metal–metal interactions in coordinative solvents, since less energetic bands should appear when the $\text{Au}\cdots\text{Tl}$ interactions remain.^{3b} Nevertheless, the poor solubility of these materials in nondonor solvents does not allow us to confirm this fact.

By contrast, as noted, complexes **1–4** display a strong luminescence in the solid state. For instance, the precursor complex $[\text{AuTl}(3,5\text{-C}_6\text{Cl}_2\text{F}_3)_2]_n$ (**1**) shows an emission at an energy similar to those previously reported for the related compounds $[\text{AuTl}(\text{C}_6\text{X}_5)_2]_n$ ($\text{X} = \text{C}_6\text{Cl}_5, \text{C}_6\text{F}_5$).² Thus, it emits at 510 nm (max. exc. at 380 nm) at room temperature, shifting the emission at 505 nm (max. exc. 370 nm) at 77 K, showing complicated emission profiles. As in the former, the emission energy of complex **1** is independent of the excitation wavelengths. The shift to high energy with decreasing temperature in the solid state, although not very common, is not unusual in extended systems bearing similar metal centers, and it has been reported to be related to the rigidity of the structure.¹²

In the case of the anionic chains, all of them behave similarly to complex **1** in solution; that is, all the complexes lose their color and optical properties, but they recover them when the solvent is evaporated. In the case of the anionic chains built up with a unique type of aryl group, they display one emission at room temperature, but show, in addition, a shoulder at 77 K (see Figure 6). Thus, $\{\text{NBu}_4[\text{Tl}_2\{\text{Au}(\text{C}_6\text{Cl}_5)_2\}\{\mu\text{-Au}(\text{C}_6\text{Cl}_5)_2\}_2]\}_n$ (**2**) and $\{\text{NBu}_4[\text{Tl}\{\text{Au}(3,5\text{-C}_6\text{Cl}_2\text{F}_3)_2\}_2]\}_n$ (**3**) show emissions at 575 (max. exc. at 430) for **2** and 500 nm (max. exc. at 410 nm) for **3**, at room temperature and at 560 (sh) and 612 nm (max. exc. at 430) for **2** and at 470 (sh) and 520 nm (max. exc. at 430) for **3**, at 77 K, respectively. In the case of the anionic complex **4**, whose structure presents both types of aryl group in the molecule, two different emissions are observed both at room temperature at 545 (max. exc. at 450) and 565 nm (max. exc. at 500 nm) and at 77 K at 580 (max. exc. at 500) and 620 nm (max. exc. at 520 nm) (Figure 7).

On the basis of the data summarized above, the assignment of the emissive states in compounds **1–4** is uncertain, because it seems to be related to the different structural arrangements that lead to a different number

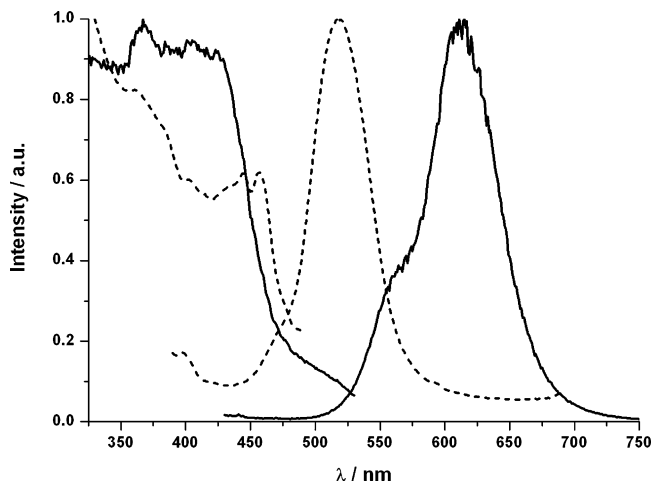


Figure 6. Normalized excitation and emission spectra of **2** (solid lines) and **3** (dashed lines) in the solid state at 77 K.

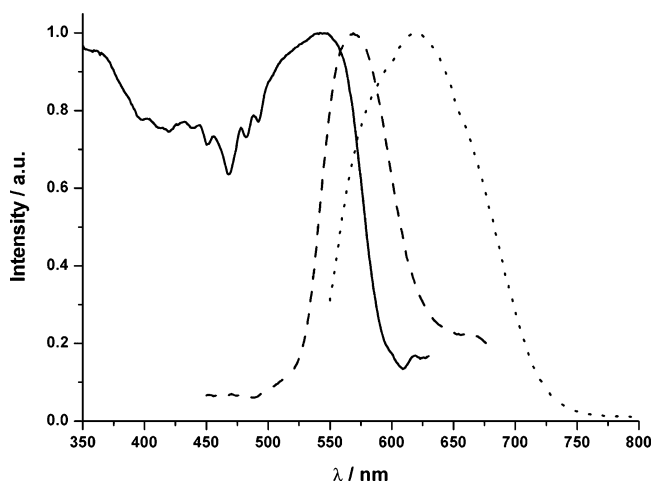


Figure 7. Normalized excitation (solid line) and emission spectra (excited at λ 500 nm (dashed line) and 520 nm (dotted line)) of **4** in the solid state at 77 K.

of $\text{Au}(\text{I})\cdots\text{Tl}(\text{I})$ interactions and also to the different aryl groups in each $[\text{Au}\cdots\text{Tl}]$ fragment in the solid state structures. Taking into account that the four complexes lose their optical properties in solution and that their spectroscopic data (NMR, IR, etc.) also suggest the breaking of the structures into ionic counterparts in solution without any sign of association, it seems likely that the gold–thallium interactions are the main contributors to the emissive excited states. For complex **1**, similarly to other extended linear chains previously reported built only by mean of Tl^+ centers and $[\text{AuR}_2]^-$ fragments,² only one emission is observed at room temperature and at 77 K; this fact is common in extended systems and is in accordance with the presence of one exciton delocalized along the chain axis.¹³ In the case of the anionic chains **2–4**, we can observe different structural arrangements and, as we mentioned in the structural analyses section, they can be described as infinite chains formed by unsupported $\text{Au}\cdots\text{Tl}$ interactions, which have incorporated a half (**2**) or one (**3, 4**)

(12) (a) Lees, A. J. *Chem. Rev.* **1987**, *28*, 4623. (b) Ferrandi, G. J. In *Elements of Inorganic Photochemistry*; John Wiley & Sons: New York, 1988. (c) Wang, S.; Garzón, G.; King, C.; Wang, J. C.; Fackler, J. P., Jr. *Inorg. Chem.* **1989**, *28*, 4623.

(13) (a) Forward, J. M.; Fackler, J. P., Jr.; Asseffa, Z. In *Optoelectronic Properties of Inorganic Compounds*; Roundhill, D. M., Fackler, J. P., Jr., Eds.; Plenum Press: New York, 1999; p 195. (b) Hao, L.; Mansour, M. A.; Lachicotte, R. J.; Gysling, H. J.; Eisenberg, R. *Inorg. Chem.* **2000**, *39*, 5529.

additional $[\text{AuR}_2]^-$ fragment per thallium. Therefore, the site selective excitation observed in these complexes at low temperature and in complex **4** also at room temperature is likely to be related to the presence of different excited states, perhaps related to different numbers of gold–thallium interactions. In fact, as it has been repeatedly reported in heteronuclear or homonuclear gold systems, as the number of metal–metal interaction increases, the band gap energy is reduced, shifting the emissions to low energy.¹⁴ Thus, accordingly with these thoughts, the high-energy bands observed are perhaps based on the new unsupported $\text{Au}\cdots\text{Tl}$ interactions formed by addition of $[\text{AuR}_2]^-$ groups to the extended chains, while the low-energy bands are likely assigned to delocalized excitons along the main axis. From the structural data, we cannot deduce any correlation between luminescence and Au–Tl interatomic distances (see crystal structure section). In addition, the participation of the perhalophenyl groups in those states cannot be excluded, since previous time-dependent DFT calculations point out the anionic $[\text{AuR}_2]^-$ fragments as the origin of the electronic transitions, with an important contribution of the perhalophenyl rings.^{2b,3a,c} Therefore, the assignment of one or two emissive excited states as an admixture of MMCT (metal (gold) to metal (thallium) charge transfer) and LMCT (ligand (perhalophenyl) to metal charge transfer) in origin is also possible.

Finally, lifetime measurements carried out for the four complexes at room temperature in the solid state gave in all cases biexponential decays of 1957 and 248 ns ($\chi^2 = 2.7$) for **1**, 54.5 and 11 μs ($R^2 = 0.9995$) for **2**, 363.6 and 146.9 ns ($\chi^2 = 3.2$) for **3**, and 595.4 and 224.2 ns ($\chi^2 = 2.2$) for **4**. The shorter lifetimes in the nanoseconds range and the small separation between excitation and emission peaks are usual in extended Au–Tl systems and assigned as fluorescence. By contrast, the longer lifetime of complex **2** could be related with the different structural disposition of the metal centers, since it can be also viewed as an association of loosely bound butterfly Au_2Tl_2 clusters joined by anionic $[\text{Au}(\text{C}_6\text{Cl}_5)_2]^-$ fragments. In this sense, a butterfly-type complex previously reported in our group showed also a lifetime in the microsecond range and it was assigned as phosphorescence.^{10a}

Experimental Section

Instrumentation. Infrared spectra were recorded in the range 4000–200 cm^{-1} on a Perkin-Elmer FT-IR Spectrum 1000 spectrophotometer using Nujol mulls between polyethylene sheets. C, H, S analyses were carried out with a Perkin-Elmer 240C microanalyzer. Mass spectra were recorded on a HP59987 A Electrospray. ^1H and ^{19}F NMR spectra were recorded on a Bruker ARX 300 in D_8 -THF solutions. Chemical shifts are quoted relative to SiMe_4 (^1H , external) and CFCl_3 (^{19}F , external). Excitation and emission spectra were recorded with a Jobin-Yvon Horiba Fluorolog 3-22 Tau-3 spectrofluorimeter. Fluorescence lifetime data were obtained with the same spectrofluorimeter operating in the phase-modulation mode.

(14) (a) Mansour, M. A.; Connick, W. B.; Lachicotte, R. J.; Gysling, H. J.; Eisenberg, R. *J. Am. Chem. Soc.* **1998**, *120*, 1329. (b) Lee, Y. A.; McGarrah, J. E.; Lachicotte, R. J.; Eisenberg, R. *J. Am. Chem. Soc.* **2002**, *124*, 10662. (c) Burini, A.; Bravi, R.; Fackler, J. P., Jr.; Galassi, R.; Grant, T. A.; Omary, M. A.; Pietroni, B. R.; Staples, R. J. *Inorg. Chem.* **2000**, *39*, 3158.

The phase shift and modulation were recorded over the frequency range 0.1–10 MHz. Phosphorescence lifetime was recorded with a Fluoromax phosphorimeter accessory containing a UV xenon flash tube with a flash rate between 0.05 and 25 Hz. The lifetime data were fitted using the Jobin-Yvon software package and the Origin 6.1 program.

General Comments. Thallium(I) hexafluorophosphate is commercially available and was purchased from Aldrich. The precursor complexes $\text{NBu}_4[\text{Au}(3,5\text{-C}_6\text{Cl}_2\text{F}_3)_2]$,⁴ $\text{NBu}_4[\text{Au}(\text{C}_6\text{Cl}_5)_2]$,¹⁵ and $[\text{AuTl}(\text{C}_6\text{Cl}_5)_2]_n$ ^{2b} were obtained according to literature procedures.

Preparation of $[\text{AuTl}(3,5\text{-C}_6\text{Cl}_2\text{F}_3)_2]_n$ (1**).** To a tetrahydrofuran solution (20 mL) of thallium(I) hexafluorophosphate (0.07 g, 0.20 mmol) was added $\text{NBu}_4[\text{Au}(3,5\text{-C}_6\text{Cl}_2\text{F}_3)_2]$ (0.168 g, 0.20 mmol). The solution was stirred for 45 min, and the solvent was removed under reduced pressure. The remaining residue was extracted with diethyl ether (40 mL) and filtered through Celite. The solvent was evaporated to ca. 5 mL, and the addition of 10 mL of *n*-hexane gave a white precipitate, **1**. The solid was filtered off and washed with *n*-hexane (2 \times 5 mL). Yield: 88%. Anal. (%) Calcd for **1** ($\text{C}_{12}\text{AuCl}_4\text{F}_6\text{Tl}$): C, 18.0. Found: C, 18.1. FT-IR (Nujol mulls): $\nu(\text{C}_6\text{Cl}_2\text{F}_3)$ at 1587, 1562, 1047, and 775 cm^{-1} . ES(+) *m/z*: 205 [^{205}Tl]⁺. ES(−) *m/z*: 597 $[\text{Au}(3,5\text{-C}_6\text{Cl}_2\text{F}_3)_2]^-$. ^{19}F NMR (THF- D_8 , room temperature, ppm): δ −88.0 (s, 2F, F_o); δ −119.1 (s, 1F, F_p).

Preparation of $\{\text{NBu}_4[\text{Tl}_2\{\text{Au}(\text{C}_6\text{Cl}_5)_2\}\{\mu\text{-Au}(\text{C}_6\text{Cl}_5)_2\}_2\}_n$ (2**).** To a suspension of $[\text{NBu}_4][\text{Au}(\text{C}_6\text{Cl}_5)_2]$ (0.094 g, 0.10 mmol) in 20 mL of toluene was added $[\text{AuTl}(\text{C}_6\text{Cl}_5)_2]_n$ (0.180 g, 0.20 mmol). The solution was stirred for 45 min, and the addition of *n*-hexane gave a yellow precipitate, **2**. The solid was filtered off and washed with *n*-hexane (3 \times 5 mL). Yield: 65%. Anal. (%) Calcd for **2** ($\text{C}_{52}\text{H}_{36}\text{Au}_3\text{Cl}_{30}\text{NTl}_2$): C, 23.5; H, 1.8; N, 0.7. Found: C, 23.3; H, 1.6; N, 0.8. FT-IR (Nujol mulls): $\nu(\text{C}_6\text{Cl}_5)$ at 836 and 614 cm^{-1} ; $\nu(\text{NBu}_4^+)$ at 881 cm^{-1} . ES(+) *m/z*: 205 [^{205}Tl]⁺, 242 $[\text{NBu}_4]^+$. ES(−) *m/z*: 696 $[\text{Au}(\text{C}_6\text{Cl}_5)_2]^-$.

Preparation of $\{\text{NBu}_4[\text{Tl}\{\text{Au}(3,5\text{-C}_6\text{Cl}_2\text{F}_3)_2\}_2\}_n$ (3**).** A suspension of $[\text{NBu}_4][\text{Au}(3,5\text{-C}_6\text{Cl}_2\text{F}_3)_2]$ (0.168 g, 0.20 mmol) in 20 mL of toluene was treated with $[\text{AuTl}(3,5\text{-C}_6\text{Cl}_2\text{F}_3)_2]_n$, **1** (0.160 g, 0.20 mmol), and stirred at room temperature. After 45 min, the addition of the same volume of *n*-hexane gave a green precipitate **3**. The solid was filtered off and washed with *n*-hexane (3 \times 5 mL). Yield: 79%. Anal. (%) Calcd for **3** ($\text{C}_{40}\text{H}_{36}\text{Au}_2\text{Cl}_8\text{F}_{12}\text{NTl}$): C, 29.3; H, 2.2; N, 0.8. Found: C, 29.4; H, 2.3; N, 0.8. FT-IR (Nujol mulls): $\nu(\text{C}_6\text{Cl}_2\text{F}_3)$ at 1588, 1561, 1047, and 776 cm^{-1} ; $\nu(\text{NBu}_4^+)$ at 881 cm^{-1} . ES(+) *m/z*: 205 [^{205}Tl]⁺, 242 $[\text{NBu}_4]^+$. ES(−) *m/z*: 597 $[\text{Au}(3,5\text{-C}_6\text{Cl}_2\text{F}_3)_2]^-$. ^{19}F NMR (THF- D_8 , room temperature, ppm): δ −87.7 (s, 2F, F_o); δ −120.6 (s, 1F, F_p).

Preparation of $\{\text{NBu}_4[\text{Tl}\{\text{Au}(\text{C}_6\text{Cl}_5)_2\}\{\text{Au}(3,5\text{-C}_6\text{Cl}_2\text{F}_3)_2\}_2\}_n$ (4**).** A suspension of $[\text{NBu}_4][\text{Au}(3,5\text{-C}_6\text{Cl}_2\text{F}_3)_2]$ (0.168 g, 0.20 mmol) in 20 mL of toluene was treated with $[\text{AuTl}(\text{C}_6\text{Cl}_5)_2]_n$ (0.180 g, 0.20 mmol) with stirring (1 h). An alternative procedure is the treatment of $[\text{NBu}_4][\text{Au}(\text{C}_6\text{Cl}_5)_2]$ (0.188 g, 0.20 mmol) with $[\text{AuTl}(3,5\text{-C}_6\text{Cl}_2\text{F}_3)_2]_n$, **1** (0.160 g, 0.20 mmol). After 2 h, the addition of 20 mL of *n*-hexane lead to the precipitation of a yellow product, **4**, which was filtered off and washed with *n*-hexane (3 \times 5 mL). Yield: 87%. Anal. (%) Calcd for **4** ($\text{C}_{40}\text{H}_{36}\text{Au}_2\text{Cl}_{14}\text{F}_6\text{NTl}$): C, 28.1; H, 1.9; N, 0.8. Found: C, 27.6; H, 2.0; N, 0.8. FT-IR (Nujol mulls): $\nu(\text{C}_6\text{Cl}_5)$ at 837 and 612 cm^{-1} ; $\nu(\text{C}_6\text{Cl}_2\text{F}_3)$ at 1587, 1560, 1047, and 776 cm^{-1} ; $\nu(\text{NBu}_4^+)$ at 881 cm^{-1} . ES(+) *m/z*: 205 [^{205}Tl]⁺, 242 $[\text{NBu}_4]^+$. ES(−) *m/z*: 597 $[\text{Au}(3,5\text{-C}_6\text{Cl}_2\text{F}_3)_2]^-$, 696 $[\text{Au}(\text{C}_6\text{Cl}_5)_2]^-$. ^{19}F NMR (THF- D_8 , room temperature, ppm): δ −87.6 (s, 2F, F_o); δ −119.6 (s, 1F, F_p).

Crystallography. Crystals were mounted in inert oil on glass fibers and transferred to the cold gas stream of a Nonius Kappa CCD diffractometer equipped with an Oxford Instruments low-temperature attachment. Data were collected using

(15) Usón, R.; Laguna, A. *Coord. Chem. Rev.* **1986**, *70*, 1.

monochromated Mo K α radiation ($\lambda = 0.71073 \text{ \AA}$). Scan type: ω and ϕ . Absorption corrections: numerical (based on multiple scans). The structures were solved by direct methods and refined on F^2 using the program SHELXL-97.¹⁶ All non-hydrogen atoms were refined anisotropically. Hydrogen atoms were included using a riding model. Further details of the data collection and refinement are given in Table 1. Selected bond lengths and angles are collected in Tables 2–4 and crystal structures of complexes **2–4** in Figures 1–5.

(16) Sheldrick, G. M. *SHELXL-97*, A program for crystal structure refinement; University of Göttingen: Göttingen, Germany, 1997.

Acknowledgment. This work was supported by the DGI(MEC)/FEDER (CTQ2004-05495). M.M. thanks CAR for a grant.

Supporting Information Available: X-ray crystallographic files in CIF format for the structural characterization of complexes **2–4**. Figures S.I. 1–3 showing thermal ellipsoid plots for the anion of complexes **2–4**. This material is available free of charge via the Internet at <http://pubs.acs.org>.

OM049021I